The Collapse of the Hanshin Expressway (Fukae) Bridge, Kobe 1995: Soil–Foundation–Structure Interaction, Reconstruction, Seismic Isolation

Gazetas, George; Anastasopoulos, Ioannis; Gerolymos, Nikos; Mylonakis, George;Syngros, Costis

Abstract

The collapse of 18 spans (total length 630 m) of the Hanshin Expressway Route 3 elevated highway bridge in Fukae during the 1995 Kobe earthquake is investigated. The overturned concrete deck was monolithically connected ("piltz" form) to 3.1-m–diameter circular–column piers, founded on 17–pile groups in alluvium sand and gravel. The collapse has been attributed by many research engineers to inadequate structural design, stemming from insufficient and prematurely–terminated longitudinal reinforcement, inadequate hoop anchorage, and (for the large intensity of shaking) insufficient shear capacity. The importance of other factors has been largely ignored. This study presents evidence in the form of a parametric study of the inelastic response of the bridge–foundation–soil system, showing that the role of Soil–Foundation–Structure Interaction (SFSI) was significant and decisively detrimental.

The extreme distress of the structure also severely affected the piles, which were found to have suffered flexural cracking near their top; lateral pile load tests confirmed the decline of their structural stiffness and strength by about 50%. But the stiffness of the pile–soil system apparently only marginally decreased and, thanks to the elaborate seismic isolation bearings introduced in the new design, no changes to foundations were deemed necessary. We show that even a much simpler friction–based seismic isolation system would have saved the original bridge with rather minor acceptable damage.

1 Introduction

The M_w7 1995 Kobe Earthquake was one of the few major earthquakes to hit from "underneath" a modern city with an extremely high concentration of civil engineering facilities. It resulted in the worst earthquake-related disaster in Japan since the 1823 M_s8 Kanto earthquake. The port of the city which was of critical importance to the Japanese

economy was left almost completely out of service, while very significant was the damage to the elevated highways which carried the traffic through the city. The overall direct economic loss was about $100 billion. See the numerous detailed reports [1, 2, 3, 4, 5].

Seismologically the Earthquake came as a surprise, primarily due to the extremely severe recorded ground motions - much stronger than in any previous recorded earthquake in Japan.

In the devastation caused by the earthquake, the collapse and transverse overturning of the 630 m section of the Hanshin Expressway elevated highway Route 3 in Fukae was perhaps the most impressive failure. This bridge and the whole of Route 3 run along the city, parallel to the shoreline. Built in 1969, it consisted of single circular columns, 3.1m in diameter and about 12m in height, monolithically-connected to a concrete deck in mushroom-like ("piltz") form, supported on groups of 16 to 17 piles. The main geometric characteristics of the bridge are depicted in Figure 1, while the longitudinal and transverse reinforcement of the collapsed pier are presented in Figure 2.

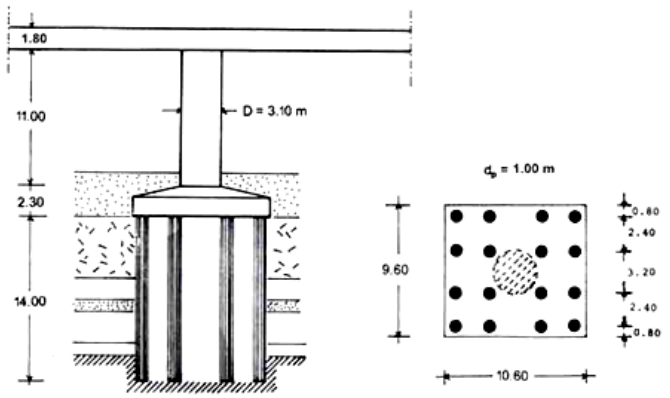

Fig. 1. Geometric characteristics of typical collapsed pier in Fukae section

Detailed investigations of the performance of Fukae section have been presented by several authors [4, 5, 6, 7, 8, 9, 10, 11, 12] who studied certain aspects of the problem to explain the inadequate (for this earthquake) structural design of the piers. They considered factors such as :

a) the inadequate transverse reinforcement in the pier

b) the inadequate anchorage of longitudinal reinforcement

c) the use of un-conservative (elastic) methods to determine design shear forces.

Quite interesting are the findings of Adachi et al [13] concerning the totally different response of two adjacent, almost identical, bridge piers during the 1995 earthquake. Both piers were situated at a bridge section near the Fukae collapsed segment. They were both practically the same size, carrying almost the same superstructure load, and designed and constructed during the same period, following the same standards and regulations. The first pier failed in shear, at the region of longitudinal reinforcement cut-off, causing the collapse of the supported span. This collapse was clearly very similar to the Fukae section collapse. The second pier suffered only minor damage, in the form of flexural micro-cracking at its bottom, surviving the earthquake. The only difference between the two piers was the longitudinal reinforcement at their base section. Both piers were reinforced with two rings of longitudinal reinforcement. But one of them had an additional (third) reinforcement ring, terminating at 2.5 m distance from the bottom. Astonishingly, the pier with this *additional* reinforcement was the one that collapsed.

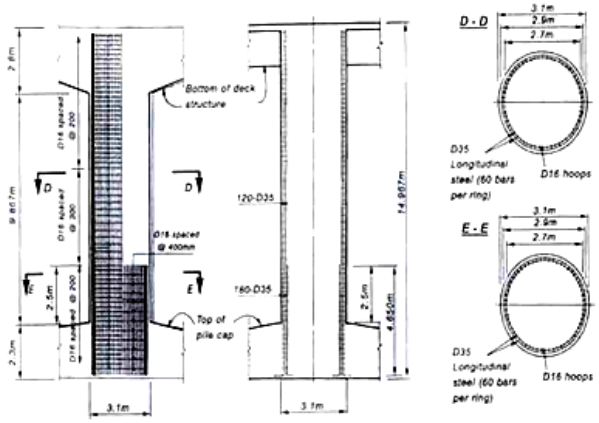

Fig. 2. Longitudinal and transverse reinforcement of typical collapsed pier

Adachi et al conducted a series of one–seventh (1/7) scale tests to verify this dramatic difference in the response of the two piers. They conducted static and cyclic tests, as well as pseudo–dynamic experiments, utilising three different ground motions. Figure 3 depicts typical cyclic test results for the two piers, as well as pictures of the damage of the tested specimens. The cyclic loading tests succeeded in reproducing the observed field performance, revealing the inherent weakness of the heavier–reinforced pier. Evidently, the additional longitudinal reinforcement *provided* additional flexural resistance to the heavily reinforced pier, but which as a result attracted a higher bending moment, M. The accompanying shear force, $Q = M/h$, was also proportionally higher. However, the shear reinforcement, and therefore the shear strength of the pier, had not been increased, and they

were thus inadequate, leading the structure to "premature" shear failure. On the other hand, the lightly reinforced pier reached its flexural capacity a little faster attracting a smaller M, and therefore the shear demand was sufficiently limited. This pier "failed", in bending, developing only flexural cracks, in contrast to the shear failure, which was brittle and lead to collapse.

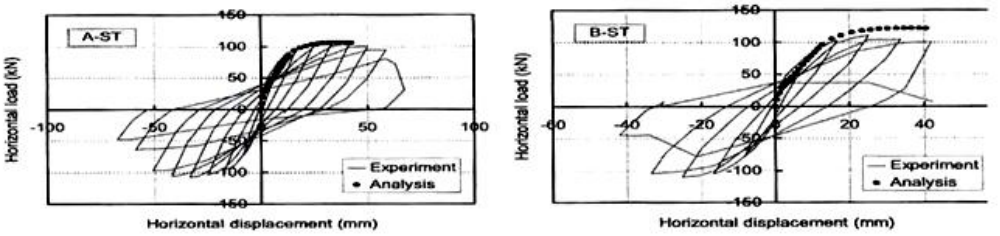

(a) A-ST

(b) B-ST

"Lightly" reinforced pier
(2 rings of uninterrupted longitudinal reinforcement)

"Heavily" reinforced pier
(2 rings of uninterrupted longitudinal reinforcement
+ 1 ring terminating at 1/3H)

(a)

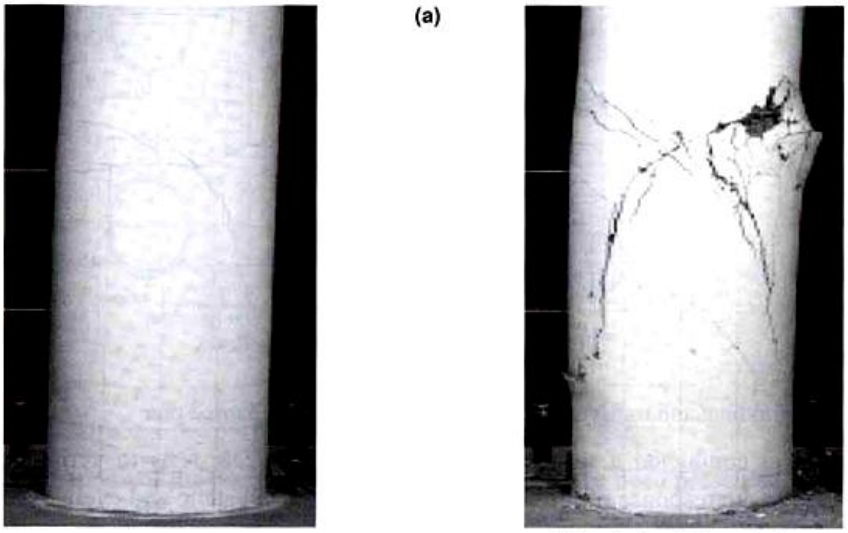

"Lightly" reinforced pier
(2 rings of uninterrupted longitudinal reinforcement)

(b)

"Heavily" reinforced pier
(2 rings of uninterrupted longitudinal reinforcement
+ 1 ring terminating at 1/3H)

Fig. 3. (a) Cyclic load-displacement diagrams for the two investigated piers, and (b) pictures of the observed damage [courtesy of Dr. Adachi et al, 2003]. The "lightly" reinforced pier was the one that survived the earthquake, as well as the cyclic loading tests, while the heavily reinforced pier, despite its higher monotonic strength, exhibited cyclic strength degradation and failed in shear.

Notwithstanding the importance of these findings, there is evidence presented in this paper that local soil conditions and dynamic interaction between foundation and superstructure further aggravated its inelastic behavior thereby contributing to the collapse.

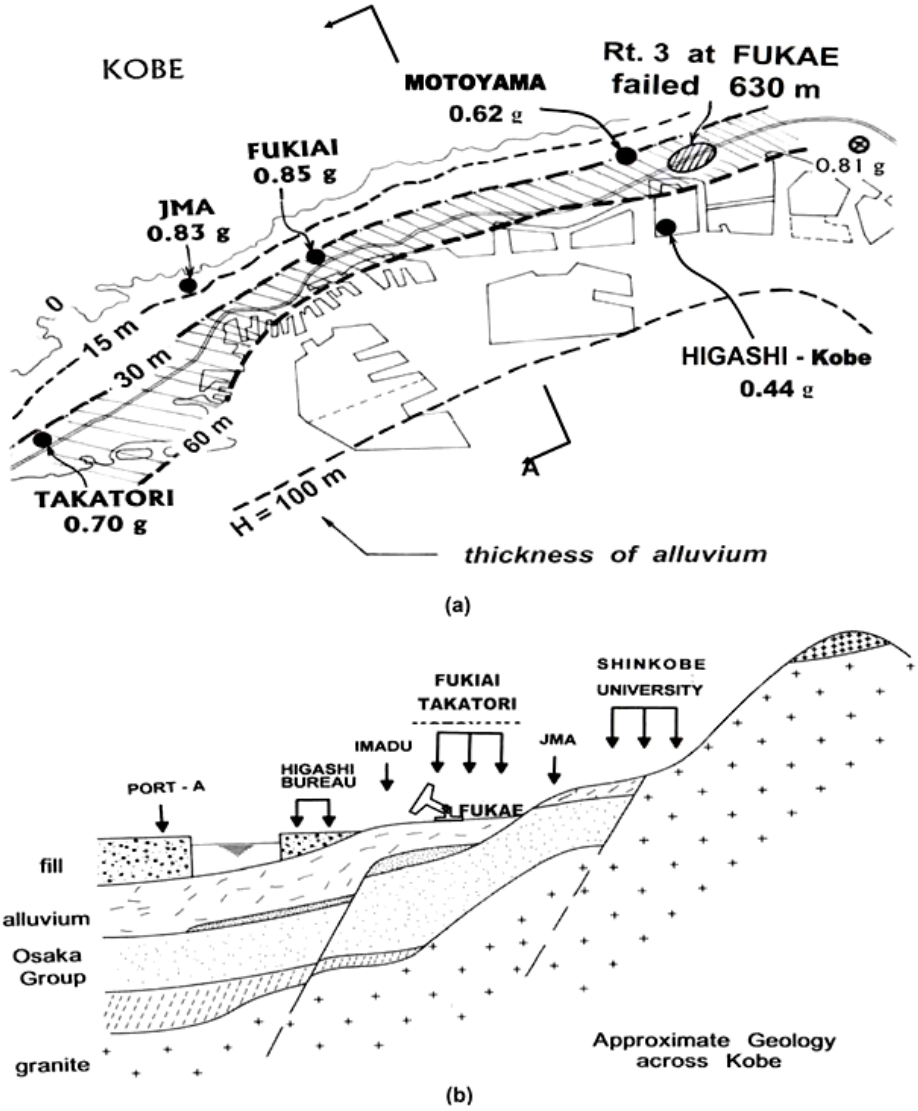

Fig. 4. (a). Contours of alluvium thickness and location of accelerometers; (b) approximate geologic section along A-A showing of the top soil groups. Notice the broad similarity in soil conditions between Fukae and the sites of Fukiai and Takatori recording stations.

An additional concern comes from the fact that soil–structure interaction (SFSI) has been traditionally considered as invariably *beneficial* for seismic response. Apparently, this perception stems from oversimplifications in the nature of seismic demand adopted in seismic code provisions. The most important of these simplifications, with reference to SFSI, are [14] : (i) use of design acceleration spectra that decrease monotonically with increasing structural period; (ii) response modification coefficients (i.e., "behavior" factors used to derive seismic forces) which are either period independent or increase with increasing structural period; (iii) foundation damping derived assuming homogeneous half-space conditions for the soil, which tends to over-predict the overall effective damping ; (iv) kinematic response coefficients for spread footings indicating that foundation response is smaller than the free-field soil motion.

This beneficial role of SFSI, although in accord with reality in many cases, has been essentially turned into a dogma. Thus, practicing engineers usually avoid the complication of accounting for SFSI, as a simplification that supposedly leads to improved safety margins. Results presented in this paper are in contrast with this perception. It is worth mentioning that detrimental effects of SFSI on seismic response have been pointed out in the past [14, 15, 16, 17, 18] ; however, these studies have not yet received the deserved attention by code writers and engineers.

The work reported in this paper involves:

- discussion of seismological and geotechnical information pertaining to the bridge site;
- analysis of free-field soil response;
- analysis of response of the foundation–superstructure system;
- evaluation of results through comparisons with earlier studies that did not consider SFSI.
- discussion and analysis of reconstruction–related problems
- analysis of the seismic response of the newly designed bridge
- analysis of the seismic response of the collapsed bridge with two hypothetical seismic isolation schemes.

2 The role of soil

2.1 Soil Effects on the Pattern and Intensity of Ground Shaking

Kobe and the towns of Asiya, Nishinomiya, and Amagasaki are built along the shoreline forming of an elongated rectangle about 30 km long and 2 to 3 km wide. The soil in the region consists primarily of sand and clay with gravel of thickness varying for 0 to 80m, underlain by stiffer neogenes and eventually soft rock. The granitic bedrock that outcrops in the mountain region bordering the city dips steeply in the northwest-southwest direction; in the shoreline it already lies at a depth of about 1 to 1.5 km. Figures 4(a), 4(b) show an approximate geological plan and cross–section of the region, as well as the locations of strong motion accelerographs.

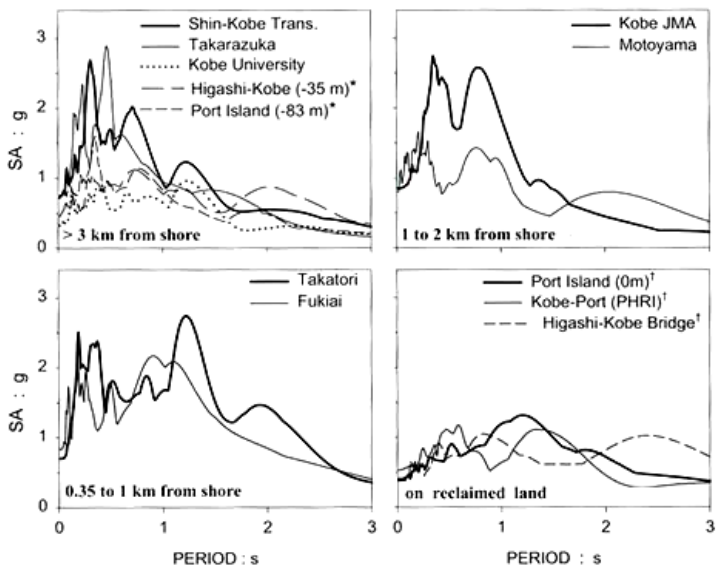

Fig. 5(a). Acceleration spectra grouped with respect to distance from the shoreline. Note the differences in predominant periods. Plotted are spectral of the fault normal components of each motion. [* denotes motions at depth; † denotes liquefied sites; $\zeta = 5\%$]

The main shock was recorded in several accelerographs, none unfortunately too close to the site. Most records were of unusually high intensity, with peak ground accelerations (PGA) and peak ground velocities (PGV) in excess of 0.80 g and 100 cm/s, respectively. PGA's in non-liquefied ground were in excess of 0.5 g throughout Kobe, Asiya, and Nishinomiya. PGA's above 0.4 g were recorded at 17 sites, while at least in three locations, PGA reached or exceeded the astounding 0.80 g.

Variability in local soil conditions among the recording stations might be partly responsible for the significant differences in the intensity and frequency content of the recorded motions, as clearly seen in Figure 4(a). Three additional effects however, have also affected the surface motions in Kobe: *forward rupture directivity*, *2D wave basin effects*, and *soil liquefaction*.

The first is of a seismological nature, affecting ground shaking at near-fault sites located in the direction of propagation of the fault rupture. The effect of forward fault-rupture directivity on the response spectrum is primarily to increase the spectral values of the horizontal component *normal* to the fault strike, at periods longer than about 0.5 sec. The resulting differences between Fault–Normal (FN) and Fault–Parallel (FP) response spectra, plotted in Figure 4(b) are indeed striking.

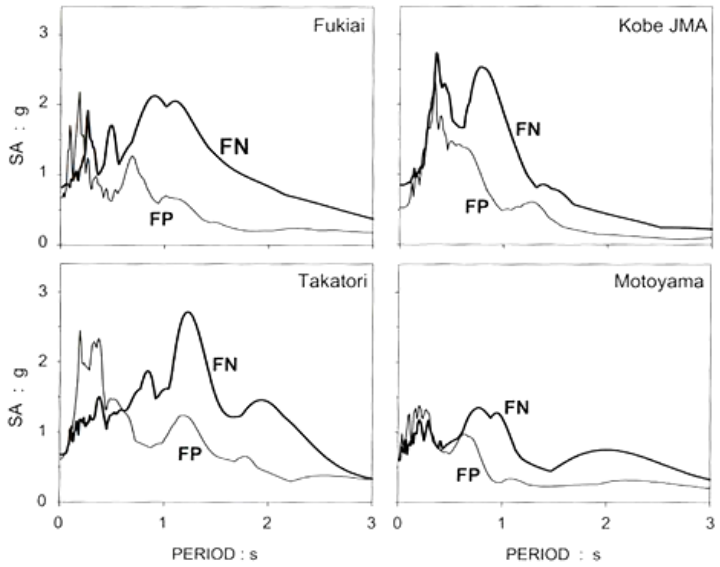

Fig.5(b).Differences between the response spectra of the fault-normal (FN) and fault parallel (FP) components of the four main records of Fig. 4(a).

The 2D basin (valley) effect stems from the constructive and destructive interference of a multitude of direct, refracted, reflected, and diffracted waves that propagate in the valley. This has been shown to increase or decrease the intensity and duration, and alter the frequency characteristics of ground motion depending on the proximity to the edge of the valley, the dipping angle, the frequency content of the excitation, and the incidence wave angles. Finally, soil liquefaction results in significant reduction of high-frequency acceleration peaks, increase of dominant period of vibration, and in large permanent deformations if static (permanent) shear stresses exist in the ground.

All these effects, have contributed (more or less) to the differences in ground motions seen in Figure 5. Evidently, the closer the site to the shore, the deeper and softer the soil deposit, thereby leading to a longer predominant period and a flatter spectrum. Interestingly, the site groups in Figure 5 differ not only with respect to distance from shore, and flexibility of soil, but also with respect to distance from the fault.

2.2 Soil–Pile–Structure Interaction

The foundation consists of 17 reinforced concrete piles having length of about 15 m and diameter of 1m, connected through a rigid cap of planar dimensions 9.6 m x 10.6 m (Figure 1). The soil surrounding the piles consists of medium dense sand with gravel. Standard Penetration Test (SPT) values for the upper 20 meters of the soil indicate low-strain shear wave velocity of the order of 200 to 300 m/s.

Structural parameters for the foundation–structure system used in previous studies are summarized in Table 1. Despite the differences in inertia and (especially) stiffness of the bridge models of the various studies, the variation in fixed–base natural period is rather small, with T_{fixed} ranging between 0.55 sec to 0.75 sec. Considering soil–structure interaction, natural period (T_{SFSI}) is somewhat longer varying between 0.75 and 0.93 seconds. Differences in pier strength are considerable with the normalized yielding strength C_y ($= F_y / M_{deck}$ g) ranging between 0.5 and 0.7, depending primarily on the value of lateral yielding force F_y. These values are quite high given the year of the design (1964). Displacement ductility capacity of the pier ranges between 1.6 to 3.2. Additional parameters in Table 1 will be discussed later on.

Detailed calculations performed by the Authors suggest a participating mass of the deck of about 1000 Mg, a rotational moment of inertia approximately 32300 Mg m^2, and a pier mass of about 226 Mg (Table 2). Following Seible et al [4], the cross-sectional moment of inertia of the cracked pier was taken at about 40% of its gross value. Using this information, the fixed-base natural period of the bridge modeled as a single-dof oscillator can be estimated using the expression [19] :

$$T_{fixed} = 2\pi \sqrt{\frac{M_{deck} + \left(\frac{33}{140}\right) M_{pier} + \left(\frac{3}{2H}\right)^2 I_{deck}}{K_{pier}}} \tag{1}$$

in which $K_{pier} = 3EI / H^3$ denotes the lateral stiffness of the pier. Eq.(1) yields:

$$T_{fixed} \cong 0.84\,s \tag{2}$$

The difference from the periods estimated by Seible et al [4] and Park [6] in Table 1 is attributed to the inclusion of the non–negligible rotational inertia of the deck.

The compliance of the foundation further increases both the natural period, T_{SFSI}, and the damping, ζ_{SFSI}, of the system. Modeling the bridge as a generalized single-dof oscillator, good estimates of natural period and damping can be obtained from the following energy-based expressions [19] :

$$T_{SFSI} = 2\pi \sqrt{\frac{M_{deck} + \phi_M M_{pier} + \phi_{21}^{\ 2} M_{cap} + \phi_{31}^{\ 2} I_{deck} + \phi_{41}^{\ 2} I_{cap}}{\phi_K K_{pier} + \phi_{21}^{\ 2} K_{hh} + \phi_{41}^{\ 2} K_{rr} + 2\phi_{21}\phi_{41} K_{hr}}} \tag{3}$$

and

$$\zeta_{SFSI} = \phi_K \zeta_{pier} + \phi_{21}^{\ 2} \zeta_{hh} + \phi_{41}^{\ 2} \zeta_{rr} + 2\phi_{21}\phi_{41}\zeta_{hr} \tag{4}$$

in which ϕ21, ϕ31, ϕ41, ϕK, and ϕM are dimensionless factors given by the expressions :

$$\phi_{21} = K_{pier}\left(K_{rr} + K_{hr}H\right)\lambda^{-1} \quad ; \quad \phi_{41} = K_{pier}\left(K_{hr} + K_{hh}H\right)\lambda^{-1} \quad ; \quad \phi_{31} = -\left[\left(1-\phi_{21}\right)\frac{3}{2H} + \frac{1}{2}\phi_{41}\right] \tag{5a}$$

$$\phi_M = \frac{1}{H}\int_0^H \psi^2 dx \; ; \; \phi_K = \frac{H^3}{3}\int_0^H \left(\frac{d^2\psi}{dx^2}\right)^2 dx \; ; \; \psi = \left(1-\phi_{21}+H\phi_{41}\right)\left[\frac{3}{2}\left(\frac{x}{H}\right)^2 + \frac{1}{2}\left(\frac{x}{H}\right)^3\right] + \phi_{21} - x\phi_{41} \tag{5b}$$

$$\lambda = \left(-K_{hr}^{\ 2} + K_{rr}K_{hh}\right) + K_{pier}\left[K_{rr} + H\left(2K_{hr} + K_{hh}H\right)\right] \tag{5c}$$

In the above equations, K_{hh} K_{rr} K_{hr}, and ζ_{hh} ζ_{rr} ζ_{hr}, denote foundation stiffness and damping in swaying, rocking, and cross swaying-rocking oscillations, respectively.

Equations (3) and (4) differ from similar formulations developed for surface footings (e.g. [20], [25]), due to the presence of cross terms K_{hr} and ζ_{hr} in the foundation impedance matrix, and the rotational inertia of deck and cap. Both features are important given the large rotational inertia of the mushroom-type superstructure *and* the presence of piles in the foundation. Note that with increasing K_{hh} and K_{rr} , Eq.(3) duly reduces to Eq.(1).

Using pertinent analytical tools from the literature [20, 21, 22] estimates of foundation stiffness have been obtained as shown in Table 2. These values refer to soil strains in the free–field of about 10^{-3}. Corresponding values at low soil strains obtained by Michaelides & Gazetas [23] are also given. The differences between the predictions, particularly in the swaying mode, are as expected.

Based on the parameters listed in Table 2, the fundamental natural period and damping ratio of the system are estimated from Eqs.(3) and (4) as

$$T_{SFSI} \approx 1.05s \quad \text{and} \quad \zeta_{SFSI} \approx 0.15 \tag{6}$$

These values are indicative of the important role of SFSI : an increase of natural period by an appreciable 20% and of damping ratio by 300 %. Note that the above values do not account for inelastic damping in the pier.

Table 1: Structural parameters used in previous studies

	Seible et al. [5]	Park [6]	Kawashima & Unjoh [8]	Michaelides & Gazetas [23]	Anastasopoulos [10]
Model	Single pier on rigid foundation	Single pier on rigid foundation	Multiple piers on flexible foundation	Single pier on flexible foundation	Single pier on flexible foundation
L (m)	12.3	12	–	11	12
E (Gpa)	-	30.1	27.8	20	25
I / I_{gross} †	0.40	0.45	0.59	0.75	1.00
K_{pier} (MN/m)	80	107	128	155	157
M_{deck}* (Mg)	1100	1121	–	1200	1100
I_{deck} (Mg m^2)	0	0	–	40000	40000
M_{cap} (Mg)	0	0	–	0	0
I_{cap} (Mg m^2)	0	0	–	0	0
T_{fixed} (s)	0.75	0.64	0.55**	0.68	0.68
T_{SFSI} (s)	-	-	0.75	0.93	0.93
F_y (kN)	5407	6640	4673	8240 (bottom)	7280 (bottom)
C_y	0.5	0.6	0.43**	0.7	0.66
force-displacement relation	-	elastic-perfectly plastic	Takeda	elastic-perfectly plastic	BIAX (Park)
ζ_{pier}(%)	-	5	–	5	5
ζ_{SFSI}(%)	-	-	–	7.5	7.5
$\mu_{capacity}$	2.4	2.2	3.2	1.6	3.6
excitation	-	JMA	JMA	JMA, Fukiai	JMA, Fukiai, Takatori
μ_{demand}	-	> 2.2	> 3.2	1.3 to 1.7	> 3.6

– = *not reported*
* *includes portion of pier mass*
** estimated by the Authors considering M_{deck} = 1100 Mg

2.2.1 Ground Shaking

The uncertainty in the characteristics of the ground motion and the soil profile at the location of the bridge dictated the use of plausible scenarios. From the nearest borehole to the site, the soil profile is judged as a relatively deep moderately-stiff to soft deposit. Five acceleration records with different peak ground accelerations and frequency characteristics are examined as plausible candidates :

- The accelerogram Fukiai, with PGA of about 0.83 g and PGV of 115 cm/s in the fault normal direction, recorded on a medium–soft and relatively deep deposit (60 m of soil with average V_s less than 400 m/s), at a distance from the presumed fault roughly similar to the corresponding distance of the failed bridge.

Table 2: Structural parameters considered in this analysis

L (m)	12				
E (GPa)	27.8				
I / I_{gross}	0.4	0.5	1	0.5	0.5
K_{col} (MN/m)	88	109	219	109	109
M_{deck} (Mg)	1000			1000	1000
I_{deck} (Mg m^2)	32300			0	0
M_{cap} (Mg)	750			750	0
I_{cap} (Mg m^2)	9000			0	0
M_{pier} (Mg)	53			53	53
K_{xx} (MN/m)	310				
K_{rx} (MN)	1090				
K_{rr} (MN m)	48300				
T_{fixed} (s)	0.84	0.75	0.53	0.62	0.62
T_{SFSI} (s)	1.04	0.98	0.84	0.89	0.87
ζ_{SFSI} (%)	9.7	10.3	12.2	10.3	10.3
$(\psi)_{fixed}$	0.72	0.72	0.73	1.07	1.07
$(\psi)_{SFSI}$	0.94	0.97	1.04	1.16	1.04

- The accelerogram Fukiai, with PGA of about 0.83 g and PGV of 115 cm/s in the fault normal direction, recorded on a medium–soft and relatively deep deposit (60 m of soil with average V_s less than 400 m/s), at a distance from the presumed fault roughly similar to the corresponding distance of the failed bridge.
- The accelerogram Takatori, with PGA of 0.70 g and PGV of 169 cm/s in the fault-normal direction, recorded on a soft and deep deposit (80 m of soil with V_s less than 400 m/s), also at a similar distance from the fault as the bridge.
- The accelerogram JMA, with PGA of 0.83 g and PGV of 96 cm/s in the fault-normal direction, recorded on a stiffer soil formation (about 10 m of stiff soil), but very close to the fault, much closer than the bridge.
- The accelerogram Motoyama, with PGA of 0.62 g and PGV of 75 cm/s recorded on a shallow soil site (soil thickness of about 20m), about 1 km to the northwest of the bridge.

- The accelerogram Higashi Kobe, with PGA of 0.44 g and PGV of 81 cm/s recorded inside a stiff layer, at a depth of 35 meters from the surface, below a liquefied layer, about 1 km south of the bridge.

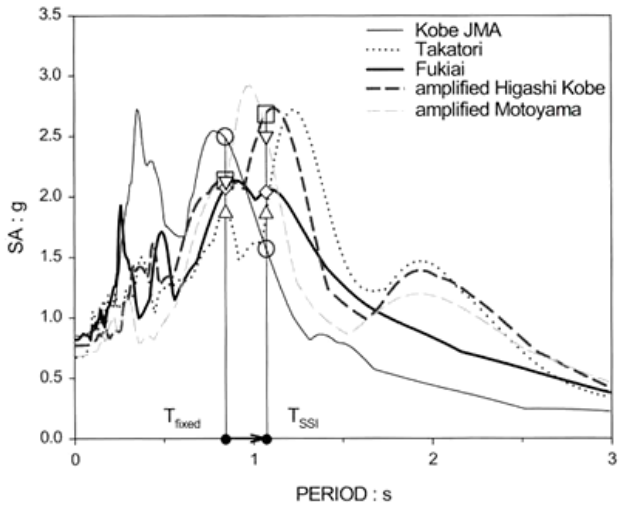

Fig. 6. Acceleration response spectra of selected ground motions in the fault normal direction; ζ = 5%. (○ for JMA ; △ for Takatori ; ◇ for Fukiai ;□ for amplified Higashi Kobe ; ▽ for amplified Motoyama)

Of the above records, the first two (Fukiai and Takatori), although recorded far from the bridge, are believed to be the most representative of the motion in Fukae Route 3 because of : (a) their roughly–similar distance from the fault, (b) the similar orientation with respect to rupture propagation, and (c) the similar soil conditions judging. The third accelerogram, the famous JMA record, was selected because it has been used by previous investigators (Table 1). However, note that It is much closer to the fault and on much stiffer soil to be representative of the Fukae motion. The last two records (Motoyama and Higashi Kobe) were selected only because of their proximity to the bridge. Owing to the very different ground conditions between these recording sites and the Fukae bridge site, the two records were suitably amplified using 1D wave-propagation theory to obtain pertinent ground surface motions. Thus, six motions were obtained and used as excitation.

Even from the elastic spectra of Figure 6, the influence of SFSI on the response starts becoming apparent. For instance, if the actual excitation was similar to the JMA record, the increase in period due to SFSI and the progressive cracking of the pier would tend to slightly reduce the response, due to the decreasing trend of the spectrum beyond about 0.8 sec (see the open circles). In contrast, with either Fukiai or Takatori motions (undoubtedly more likely surrogate motions to the unknown real ones), SFSI would initially lead to

similar response which may further progressively increase as cracking softens the structure. This is particularly true with the Takatori excitation, the response spectrum of which increases significantly beyond $T = T_{SFSI}$. The trend becomes more apparent with the Higashi-Kobe amplified record (site thickness of 50m), for which elastic response at T_{SFSI} may exceed 2.5 g, and with the Motoyama amplified record.

As a first approximation, for the somewhat conservative estimate :

$$SA \approx 0.93 \times 2.1 \text{ g} \times (5/9.5)^{0.4} \approx 1.47 \text{ g},$$

which is derived from the Fukiai record and accounts for both, the modal participation factor of the generalized system and the increased damping (from 5% to 9.5%) due to SFSI, the force reduction factor based on a calculated strength ratio, C_s, of the column of about 0.5 would be equal to approximately $1.47 / 0.5 \approx 3$. Taking the *equal displacement* rule as a first crude approximation, the ductility demand on the system would be :

$$\mu^{(s)}_{demand} \approx R \approx 3 \tag{7}$$

The ductility demand on the *pier*, $\mu^{(p)}_{demand}$, is obtained by considering only pier deformations. For an elastic–perfectly plastic system, this can be done using the expression of Mylonakis & Gazetas [18]

$$\mu^{(p)}_{demand} = (1+c)\mu^{(s)}_{demand} - c \tag{8}$$

where c is a dimensionless factor expressing the relative flexibility between foundation and superstructure :

$$c = K_{pier}\frac{H^2 K_{kk} + 2HK_{kr} + K_{rr}}{K_{kk}K_{rr} - K^2_{kr}} \tag{9}$$

For the problem at hand, c ≈ 0.7; thus,

$$\mu^{(p)}_{demand} = (1+0.7)\times 3.1 - 0.7 = 4.3 \tag{10}$$

which is 40% higher than the system ductility and exceeds by far the ductility capacity of the pier (Table 1).

On the other hand, ignoring SFSI, and for the conservative value of

$$SA \approx 0.72 \times 2.1 \text{ g} = 1.51 \text{ g}$$

which accounts for the participation factor of the generalized system in Table 2, the spectra of Figure 6 would yield a ductility demand of

$$\mu^{(p)}_{demand} \approx R = \frac{1.51}{0.5} = 3 \tag{11}$$

which, although conservatively estimated, does not exceed the possible upper–bound of ductility capacity, 3.2, suggested by Kawashima & Unjoh [8, 9] and, thereby, could hardly explain the spectacular failure of the bridge.

Although a crude first approximation, the above results indicate that the role of soil in the collapse could have been triple: *First, the soil* modified (in 1D or 2D fashion) the seismic waves so that the frequency content of the surface motion at the site became disadvantageous for the particular structure (i.e., similar to Fukiai or Takatori, rather than JMA). *Second*, the compliance of soil at the foundation increased the period of the system and moved it to a spectral region of stronger response and hence higher inertia. *Third*, ductility demand in the pier increased compared to that of the overall system, as suggested by Eq.(9).

3 Non-linear inelastic analyses

To gain further insight on the importance of SFSI on the inelastic performance of the bridge, a series of non-linear inelastic analyses were conducted using the numerical codes *DRAIN-2DX* and *ABAQUS*. To this end, a multi-degree of freedom (m–dof), Inelastic model of the pier was developed, with the column divided into four two-noded inelastic beam elements, each having one translational and one rotational degree of freedom at each end. Concentrated plasticity at the ends of the elements was adopted. The compliance of the foundation was modelled using a series of springs and dashpots attached to the base of the pier. Assuming initial yielding 2.5 m above the cap, a yielding force of 5,636 kN was established, corresponding to a yield deck acceleration of about 0.5 g. The inherent (non-SFSI) damping of the structure was assumed of the Rayleigh form, taken equal to 5% of critical. The SFSI dashpots at each degree of freedom were computed from the linear coefficients ζ_{ij} of the foundation impedance, at the characteristic period T_{SFSI}. Eigen value analyses provided the values $T_{fixed} = 0.88\,\text{sec}$ and $T_{SFSI} = 1.07\,\text{sec}$ which are in good agreement with the results of the simplified model in Table 2. Results obtained with five earthquake records are depicted in Table 3.

For the JMA record SFSI plays a beneficial role, as column ductility demand decreases from 2.5 for the fixed-base pier to 2.2 for the flexibly supported one. In contrast, with FUKIAI and Takatori motions, SFSI is clearly detrimental, increasing substantially the ductility demand in the pier. Figure 7 compares the response of the fixed system with the one that takes account of SFSI, subjected to the Fukiai record. The differences in terms of the illustrated moment-curvature diagrams are evident : SFSI is clearly detrimental. In the case of the Fukiai record, the agreement between the numerical results and those in Eqs.(11) and (12) is encouraging for the simple analysis. The strongest SFSI effect is observed with

the Takatori record: it increases from 3.2 for the fixed-base structure to the astonishing 7.3 for the flexibly supported–a somewhat furtuitious consequence of the strong peak at about T ≈ 1.2 seconds.

Table 3: Tabulated results from DRAIN-2DX and simplified analyses of the inelastic bridge response

Excitation	Pier Ductility Demand		Increase (%)		Role of SFSI	Predicted Performance
	Fixed–Base (A)	Deformable Base (B)	DRAIN-2DX (columns A, B)	Simple model (Eqs. 8 to 11)		
Fukiai	3.1	4.1	+ 32	+ 41	detrimental	failure
Takatori	3.2	7.3	+ 128	+ 46	very detrimental	failure
Motoyama†	3.5 - 3.7	3.2 - 3.5	- 5 to - 9	- 9 to + 62	≈ minor	probably failure
Higashi†	3.9 - 4.6	4.8 - 6.4	+ 23 to + 39	- 8 to +91	detrimental	failure
JMA	2.5	2.2	- 12	- 9	slightly beneficial	heavy damage

† Amplified to account for soil effects

Substantial increase in ductility with SFSI is also observed with the amplified Higashi–Kobe motion, while with Motoyama its role is rather minor. The ranges in computed ductility values for the Motoyama and HigashI stem from the different scenarios of soil thickness used in the amplification analyses. Again, the trends obtained with the simple analysis are qualitatively corroborated with the numerical study.

The excessive seismic demand computed with Fukiai, Takatori, And Higashi–Kobe records may explain the spectacular failure of the 17 piers of the bridge, especially if one considers the simultaneous deleterious action of the cyclic ***shear force*** in the cracked and plastically deforming column cross–section. This suggests that the actual excitation at the site may have indeed resembled the Fukiai, Takatori, or amplified Higashi–Kobe motions much more than the JMA or amplified Motoyama accelerograms. SFSI would, in any case, have played its important role.

4 Reconstruction – Seismic Isolation

4.1 Reconstruction : The Pile Problem

The closure of the elevated highway had severe implications for the city of Kobe. All the traffic had to pass through the surficial arteries, delaying the reconstruction work all over the city. Especially in the case of the Fukae section of Route 3, its overturning collapse did not only lead to the closure of the elevated highway, but also partly of the surficial Route

43, above which Route 3 had been built (Figure 8). Consequently, it was imperative that the whole reconstruction process would be as fast as possible. To this end, special techniques were employed to facilitate the swift removal of the failed superstructure debris. After this had been done could the reconstruction of the bridge begin. The collapsed Fukae section was replaced by a totally new design, incorporating large "shear walls" and seismic isolation. However, before proceeding to the replacement of the superstructure, the integrity of the piled foundation had to be evaluated.

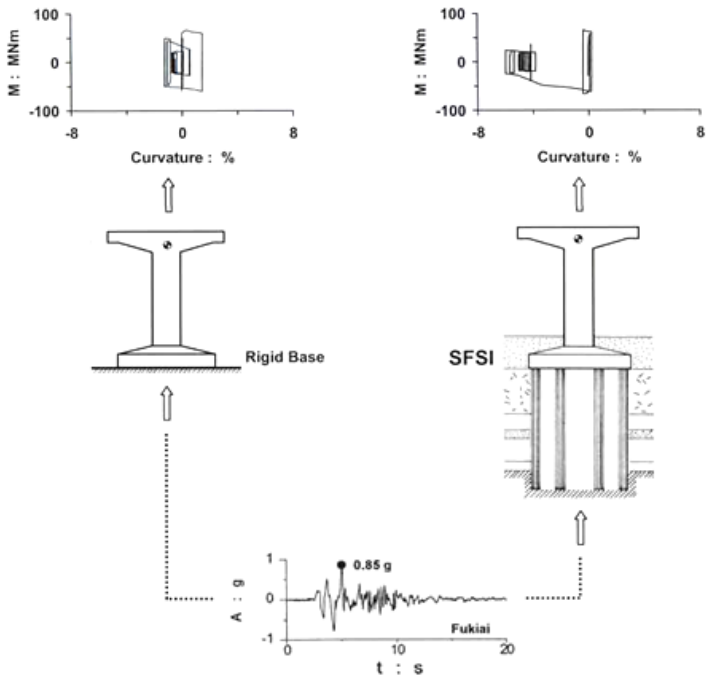

Fig. 7. Moment-curvature time-histories computed with and without SFSI, for the Fukiai record.

The replacement of the piled foundations is an extremely time-consuming operation. The removal of the damaged piles is by itself a formidable task. In fact, it is far easier to add new piles rather than to replace those damaged. But usually there are several restrictions making this impractical. As depicted in Figure 9a, in general, when installing new piles under an existing (undamaged) deck, space limitations make the use of special "mini" cranes and short reinforcement cages necessary. In Fukae this was not the case : both the piers and the deck were gone, and the field was free (in the vertical sense). The delay from the removal operations however would have been unacceptable. If the pile-integrity investigation had concluded that the piles were severely damaged, then one possible

solution would be to add new additional piles in the perimeter. As illustrated in Figure 9b, in such a case, in addition to having to excavate and construct a retaining structure around the pile head, the surficial artery (Route 43) would have remained at least partly closed for a significant period of time.

Fig. 8. The Collapse of the Fukae section did not only cause the closure of the elevated highway, but also of the surficial arteries.

To investigate the integrity of the piles several techniques were employed, including the pile integrity test, visual inspection of excavated piles, borehole photography, and slope inclinometer. In the case of the Fukae section, it was decided to conduct a lateral pile load test. As shown in Figure 10, the soil surrounding the piles was excavated down to a depth of about 4 m underneath the pile cap. After inspecting the piles, one of them was cut and horizontally loaded through a hydraulic piston. Most of the piles were found to have flexural cracks at their top, while the measured force–displacement diagram (Figure 10) revealed that their stiffness had been reduced to almost half of the theoretical (design). Despite this rather discouraging result, Hanshin Expressway decided neither to replace the piles nor to add new piles, and proceeded in the reconstruction making use of the existing "injured" pile foundations.

In view of the cautious approach and the conservative philosophy followed in the reconstruction by the Hanshin Expressway, the above decision might seem at first glance as paradoxical. It is thus worth trying to interpret the load–test results a little more carefully. Since for the load test the pile was freed from the confining soil, the measured stiffness refers to the pile itself (as a structural beam) and not to the pile–soil system. According to Gazetas [24], the lateral stiffness of a single pile embedded in soil is analogous to the power m of the structural stiffness :

$$K_H \propto (E_p I_p)^m \tag{12}$$

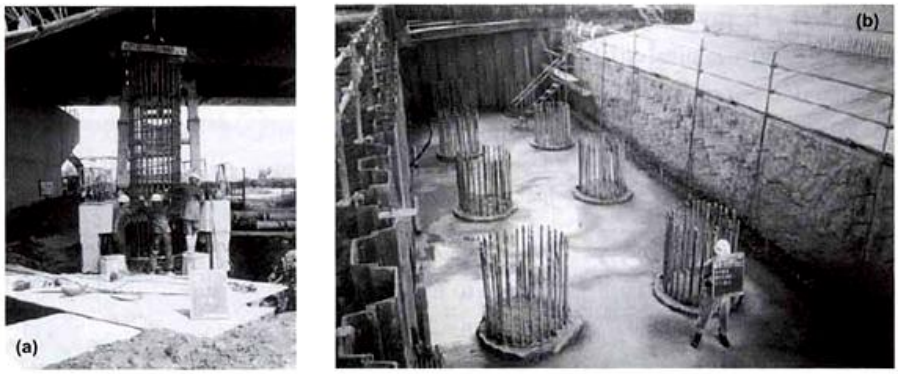

Fig. 9. (a) Space limitations when installing new piles underneath a bridge deck : requires special "mini" cranes and short reinforcement cages, (b) addition of new piles in the perimeter of the pile cap : requires the closure of the ground highway

The value of the power m depends on the variation of the soil stiffness (Young's modulus E_s) with depth. As depicted in Figure 11, while for the case of the structural unconfined beam $m = 1$, in the case of homogeneous soil $m = 0.21$. If we realistically adopt a parabolic distribution of E_s with depth, then the power m would be equal to 0.28. Therefore, for the observed reduction in *structural* stiffness :

$$[E_p I_p]_{damaged} \approx (0.50)[E_p I_p]_{initial} \tag{13}$$

The stiffness reduction of the damaged *pile*, would be proportional to :

$$(K_H)_{damage} \approx (0.50)^{0.28} (K_H)_{initial} \approx 0.82 (K_H)_{initial} \tag{14}$$

implying a reduction of less than 20% in their lateral stiffness. On the other hand, the bending stiffness of a single pile is proportional to a power q of the structural stiffness :

$$K_M \propto (E_p I_p)^q \tag{15}$$

with q ranging from 0.75 for homogeneous soil, to 0.77 for a parabolic distribution of E_s with depth. Consequently, the stiffness reduction of the damaged pile is :

$$(K_M)_{damage} \approx (0.50)^{0.77} (K_M)_{initial} \approx 0.59 (K_M)_{initial} \tag{16}$$

implying a reduction of about 40% in their bending stiffness, which however is of small significance for this large–number of piles group. Finally, the vertical axial stiffness of a single pile is :

$$K_V \propto (E_p A_p)^n \tag{17}$$

with the power n being in the order of 0.50 [22]. Since the flexural cracking of the pile is responsible for the flexural stiffness reduction, it is logical to expect the axial structural stiffness also decreased. If D is the original pile diameter, and D_r the effective diameter of the pile after flexural cracking, then the ratio of the damaged to the original flexural stiffness will be proportional to D_r^4 / D^4. For a flexural stiffness ratio of 0.50, one obtains :

$$\frac{D_r}{D} = (0.50)^{0.25} = 0.84 \tag{18}$$

The axial structural stiffness is proportional to the cross−sectional area of the pile and thus:

$$[E_p A_p]_{damaged} = \left(\frac{D_r}{D}\right)^2 [E_p A_p]_{initial} \approx (0.71)[E_p A_p]_{initial} \tag{19}$$

Thereby, according to Eqn. 15 :

$$(K_V)_{damage} \approx (0.71)^{0.5} (K_V)_{initial} \approx 0.84 (K_V)_{initial} \tag{20}$$

implying a reduction of merely about 15% in their axial stiffness.

Taking into account the fact that the inertial shear force and overturning moment on the pile cap are resisted primarily by horizontal shear and vertical normal forces, respectively, it is concluded that the loss of stiffness of the pile group in the earthquake was of the order of not more than a mere 20%. The reader should not be surprised at this small decrease : the creation of a plastic hinge at the base of the column significantly limited the transmitted loads onto the foundation . In any case the decision of Hanshin expressway was justified

4.2 The Solution Adopted by Hanshin Expressway.

As shown in Figure 12, the cylindrical piers were replaced by large orthogonal 6.0 m x 3.0 m “shear walls”. In addition, the monolithically connected to the pier concrete deck was replaced by a steel structure, seismically−isolated from the supporting pier.

The dynamic performance of the new design has been explored by Anastasopoulos [10]. The pier is found to possess an ultimate capacity $F_y \geq 15\,000$ kN, leading to a strength ratio, C_y, of at least 1.50. Its huge stiffness would lead to a period $T_{fixed} = 0.20\,\text{sec}$, if the deck had not been seismically−isolated. Taking SFSI into account, and following the logic of § 2, the period of the system would become $T_{SFSI} = 0.55\,\text{sec}$, for which Figure 6 shows that most response spectra are about 1.5 g. And since the ductility capacity of the new pier is found to exceed 5, the new pier would not collapse in a repeat of the Kobe earthquake even if the

deck had not been seismically isolated. In fact, accepting that C_y = 1.5, a spectral acceleration as high as 1.5 x 5.0 = 7.5 g would be needed to lead to collapse!

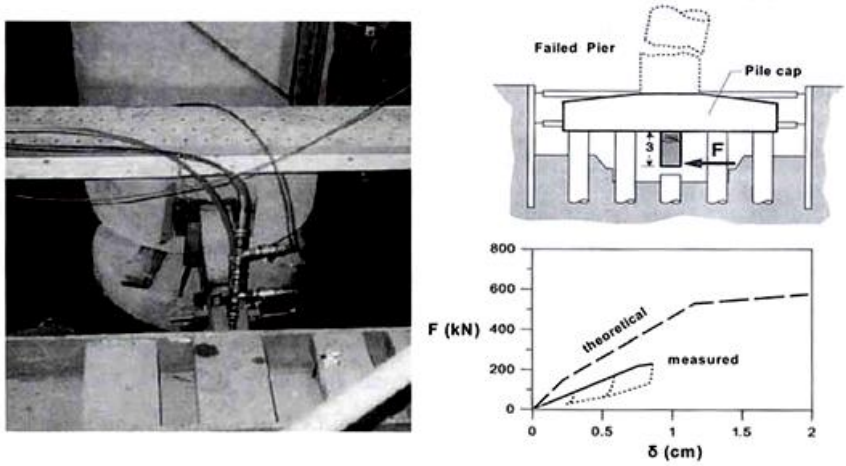

Fig. 10. In-situ measurement of the lateral stiffness of the piles : the stiffness was measured to be roughly half of its theoretical (design) value. However, it was decided to neither replace the piles nor add additional ones [photo courtesy of Y.Adachi].

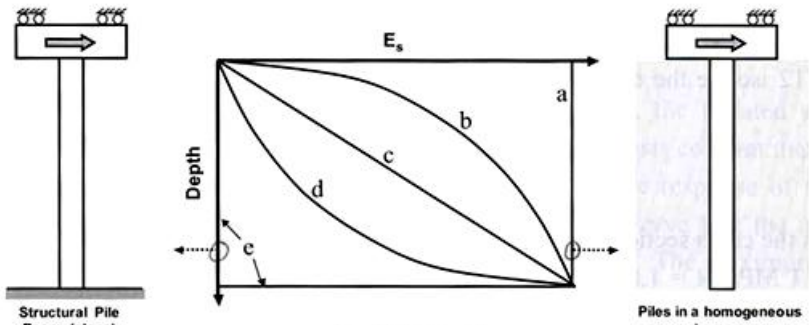

$$K_H \propto (E_p I_p)^m$$

Symbol	$E_s = E_s(z)$	m
a	homogeneous	0.21
b	parabolic	0.28
c	linear	0.35
d	hyperbolic	0.53
e	Without Soil	1.00

Fig. 11. Lateral Stiffness K_H of a single fixed-head pile with respect to the type of variation of soil stiffness (Young's modulus, E_s) with depth. Since the stiffness of the damaged pile was measured to be half of the initial value ($[E_p I_p]_{damaged} = 0.5[E_p I_p]_{initial}$) then assuming parabolic distribution of E_s would only lead to a stiffness reduction analogous to $0.5^m = 0.5^{0.28} = 0.82$, i.e. a reduction of less than 20%.

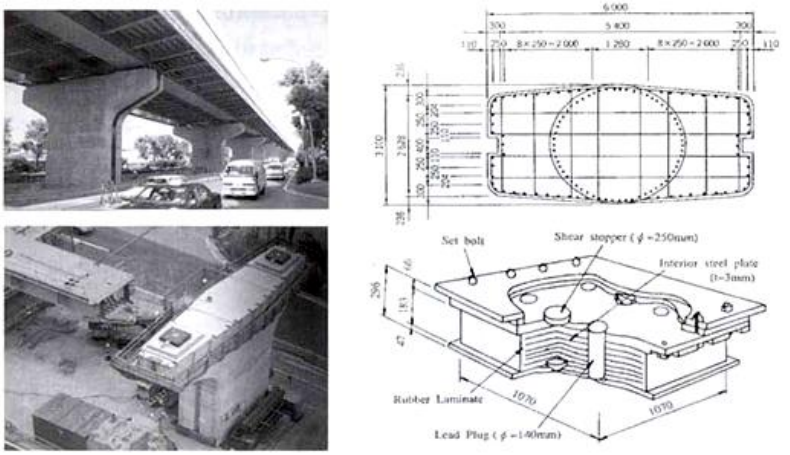

Fig. 12. The retrofitted Fukae section: New gigantic piers (3.1 m x 6.0 m) and seismic isolated superstructure through high–damping (ζ = 10 - 20%) Lead-Rubber Bearings.

However, seismic isolation was also utilised by Hanshin Expressway, presumably for two technical reasons : (a) to reduce the horizontal force and overturning moment onto the "injured" piled foundation, and thus avoid the risk of further pile damage, and (b) to completely minimize the likelihood that the pier will suffer even minor damage. The social necessity for an over-design is not discussed herein. Two Lead Rubber Bearings (LRB) seen in Figure 12 isolate the two beams of the deck from the pier. The stiffness of the LRBs is given by :

$$K_{LRB} = \frac{2GA}{h} \tag{21}$$

where A is the cross sectional area, h the effective height, and G the effective shear modulus. With $G \approx 1$ MPa, $A = 1.07^2$ m^2 , and $h = 0.183$ m, $K_{LRB} = 12.5$ MN/m. The stiffness of the system is then obtained from :

$$K_{isolated} = \frac{K_{pier}\, K_{LRB}}{K_{pier} + K_{LRB}} \tag{22}$$

With $K_{pier} = 1608$ MN/m, and $K_{LRB} = 12.5$ MN/m, the stiffness of the system is $K_{isolated} = 12.4$ MN/m, hardly affected by flexibility of the pier. The period of the isolated structure then becomes:

$$T_{isolated,fixed} = 2\pi\sqrt{m / K_{isolated}} \approx 2 \text{ sec} \tag{23}$$

Taking account of SFSI (according to § 2.2) the period of the system now increases only marginally to $T_{isolated,SFSI} \approx 2.10$ sec. Going back to Figure 6, we observe that for all the

records the corresponding spectral accelerations are between 0.90 g and 1.3 g. So, the isolated structure would behave linearly, without any damage.

4.3 Alternative Hypothetical Isolation Systems

A logical question that arises is what would have happened if the deck of the original bridge were seismically isolated, even if only partially. Following the logic of Equations 21 to 23, and assuming that the same LRB isolators had been introduced, we find that the period of the original bridge would be equal to $T_{isolated,SFSI} \approx 2.10$ sec. As in Section 2, a first approximation of the spectral acceleration for the Fukiai excitation is:

$$SA \approx 0.8 \text{ g } (5/10)^{0.4} \approx 0.61 \text{ g}$$

Accepting that $C_y = 0.5$, the ductility demand would be equal to :

$$\mu^{(p)}_{demand} \approx (0.61)/(0.50) = 1.22$$

Alternatively, following Equations 9, 10, and 11, the ductility demand on the pier :

$$\mu^{(p)}_{demand} \approx 1.35$$

Both estimates are well below the ductility capacity of the pier (Table 1: worst estimate $\mu_{capacity} = 2.2$).

To confirm the validity of the above simplified computations, the isolated system was analysed numerically. The results of the non-linear inelastic analysis confirm that the bridge would not have failed if its deck were seismically isolated. The response of the system, subjected to the Fukiai record, is depicted in Figure 13(a). Observe that the acceleration reaches 0.64 g, which is very close to the former approximation. The maximum curvature does not exceed 0.1%, a value indicative of moderate straining. However, the relative displacement between pier and deck would have reached 55 cm. Our analysis does not take into account the possibility of LRB failure. Given that the height of the LRB is 18 cm, a relative displacement of 55 cm would cause shear deformations slightly higher than 250 %, which is a large value but still below the ultimate deformation limit. This means that the LRB might have sustained some acceptable damage in such a case. So, the bridge would have survived the earthquake with some half–a–meter maximum lateral displacement and its LRBs inelastically deformed — not an unacceptable damage, in midst of the unprecedented devastation of January 17, 1995.

The Fukae section was built in 1969, a time at which the LRB technology had not yet been developed, let alone established. However, sliding bearings were widely used much earlier in bridge supports for accommodating temperature–induced deformations. It is interesting to

note that the bridges of Route 3 adjacent to the collapsed Fukae section survived the earthquake with only minor pier damage. The "temperature" bearings were seriously damaged and the deck exhibited permanent displacements of the order of 30 cm. Piers and foundation of both sections were practically identical. The only difference was the connection of the deck to the pier. Contrary to the Fukae section, where pier and deck were monolithically connected, the deck of the unharmed section was simply supported through a pin bearing and a friction bearing. The compliance of the support after the failure of the pinned bearings and thanks to the slippage on the frictional bearings allowed the superstructure to seismically "isolate itself", protecting the piers from serious failure. When the deck is simply supported exclusively through slider bearings it tends to follow the pier only if the acceleration is a small fraction of gravity, less than the friction coefficient, μ. Thus the slider limits the inertia forces of the superstructure that are transmitted on the pier.

The seismic isolation using low friction sliding bearings, with $\mu \leq 0.05$, is a relatively new technology. However, simple sliding bearings with higher coefficient of friction were surely available at the time. As shown in Figure 13(b), such a partial isolation would most likely have saved the bridge. This kind of isolation would not aim at isolating the bridge completely; for that purpose low friction sliding bearings would be needed. It simply acts as a "fuse" protecting the structure only from accelerations much higher than design. By comparing the two analysed cases of seismic isolation, it becomes evident that a "fuse"-type isolation performs at least as well as LRB. Even the permanent displacement, which is usually the main problem of such solutions, is limited to merely 15 cm. Observe that the pier behaves elastically, while with the LRB some inelasticity (leading to minor pier cracking) might have taken place. Thus, the "fuse"–protected bridge would suffer no structural damage, provided of course that the seating of the deck was large enough to accommodate the half a meter of peak displacement. In addition, some "re-centering" of the deck would have to be accomplished after the earthquake.

5 Conclusions

Analytical and recorded evidence is presented on the likely triple detrimental role of soil in the collapse of Hanshin Expressway at Fukae. *First*, the soil modified the incoming seismic waves such that the resulting ground surface motion became very severe for the particular bridge. *Second*, the presence of compliant soil in the foundation led to an increase in natural period of the bridge, to a spectral region of stronger response. *Third*, ductility demand in the pier was higher than the ductility demand of the system, as suggested by Eq. (9). All three phenomena might have simply worsened an already dramatic situation for the bridge due to: *(i)* its proximity to the fault and the ensuing strong forward–rupture directivity effects that

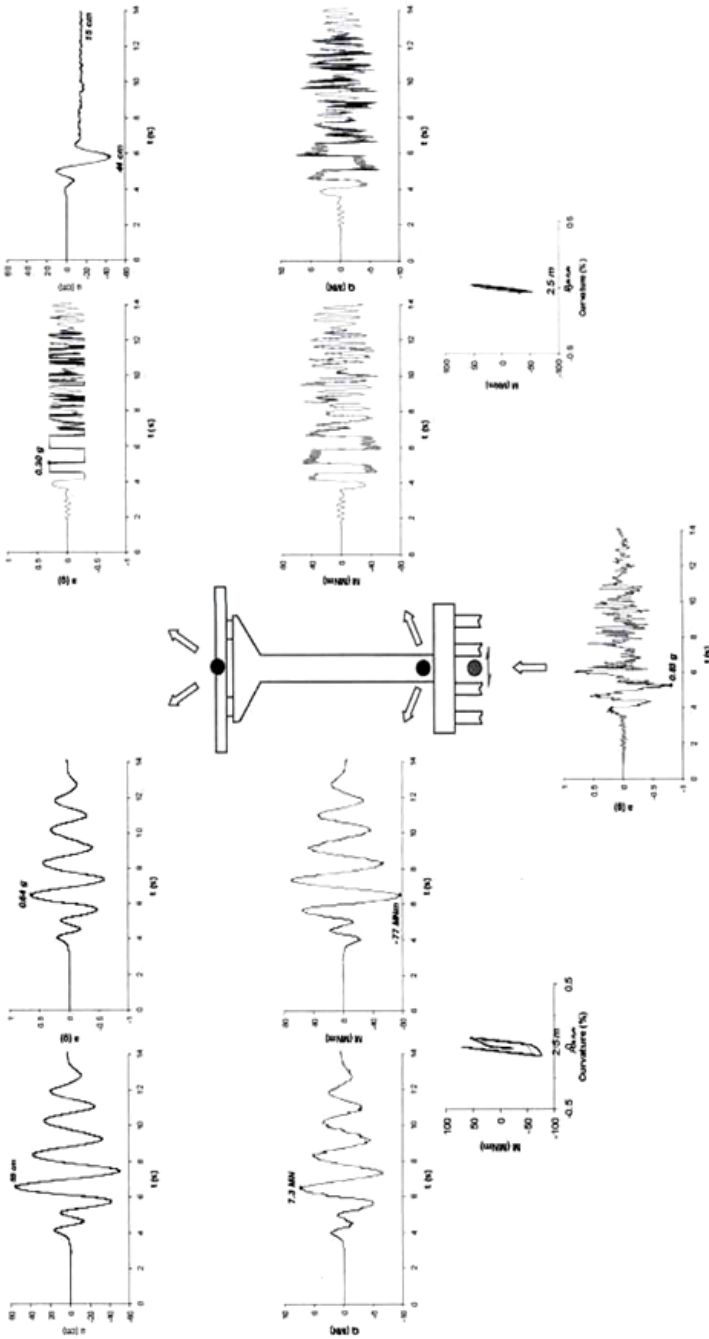

(a) LRB (b) "fuse"-type

Fig. 13. Dynamic response of the collapsed bridge with two types of hypothetical seismic isolation, subjected to the Fukiai 1995 record: in both cases the bridge would have survived, although not completely intact.

produced very high long–period acceleration pulses normal to the fault [25], which is almost in the transverse direction of the bridge ; and *(ii)* the structural deficiencies of the pier which were almost unavoidable given the time of design and construction of the bridge (1969-1970). As recently proven by the researchers of Hanshin Expressway, (Adachi et al [13]), perhaps, the main structural deficiency of the bridge was its accidental "violation" of what is currently known as capacity design, a concept that was not recognised in the 1960 s. Had the bridge been designed according to the current understanding, i.e. designed to fail in flexure and not in shear (with the same longitudinal reinforcement, but with heavier transverse shear rebars; or with the same shear reinforcement, but with less longitudinal reinforcing), it would possibly have withstood the earthquake with substantial damage but no collapse. On the other hand, this paper presents evidence suggesting that the bridge would not have collapsed if it had been seismically isolated. If *LRBs* were utilised to isolate the structure, the bearings might have been appreciably distressed and the pier might have experienced some flexural cracking. Had the bridge been isolated partially with high–friction ($\mu \approx 0.30$) "fuse"-type sliding bearings it would most probably have survived the earthquake with no visible damage other than a permanent offset of the deck of not more than about *20 cm*.

Acknowledgments

We are thankful to Dr. Takashi Tazoh of Shimizu's Institute of Technology, and to Dr. Yukio Adachi, of Hanshin Expressway, for their valuable help over several years on many aspects of our research effort.

References

[1] Committee of Earthquake Engineering, The 1995 Hyogo-Ken Nanbu earthquake–Investigation into damage to civil engineer structures, Japan Society of Civil Engineers, 1996.

[2] Japanese Geotechnical Society : Geotechnical aspects of the January 17, 1995 Hyogoken-Nambu earthquake. Soils and Foundations, Special Issue, Jan. 1996.

[3] Earthquake Engineering Research Institute : "The Hyogo-Ken Nanbu earthquake, January 17, 1995". Preliminary EERI Reconnaissance Report, 1995.

[4] Seible, F., Priestley, M.J.N. and MacRae, G. : "The Kobe earthquake of January 17, 1995; initial impressions from a quick reconnaissance". Structural Systems Research Report-95/03, University of California, San Diego, 1995.

[5] Gazetas G.: Soil Dynamics and Earthquake Engineering: Case Histories. Symeon Publishing Co, 1996, (in Greek).

[6] Park, R.: "An Analysis of the failure of the 630 m elevated expressway in Great Hanshin Earthquake". Bulletin of the New Zealand National Society for Earthquake Engineering, 29, 2, 1996.

[7] Iwasaki T., chm, et al : "Report on Highway bridge damage caused by the Hyogo–ken Nanbu Earthquake of 1995". Report by the Committee on Highway Bridge Damage, Japan, 1995.

[8] Kawashima K. & Unjoh S.: "Impact of Hanshin/Awaji earthquake on seismic design and seismic strengthening of Highway bridges". The 1995 Hyogoken–Nanbu Earthquake, Committee of Earthquake Engineering, JSCE, pp. 135–163, 1996.

[9] Kawashima K. & Unjoh S.: "The Damage of Highway Bridges in the 1995 Hyogo-*Ken Nanbu earthquake and its impact on Japanese Seismic Design*". *Journal of Earthquake Engineering, Vol. 1, No 3, pp. 505-541, 1997.*

[10] Anastasopoulos, I.: "Analysis of the failure of two bridges in the 1995 Kobe earthquake, and the role of soil". Diploma Thesis, National Technical University, Athens, Greece, 1999.

[11] Sun, L., Goto, Y., Hayashi, H. and Kosa, K.: "Damage mechanism analysis of RC bridge by nonlinear dynamic simulations". 12th World Conference on Earthquake Engineering, Paper 0488New Zealand, 2000.

[12] Abe, S., Fujino, Y. and Abe, M.: "An Analysis of damage to Hanshin Elevated Expressway during 1995 Kobe earthquake". 12th World Conference on Earthquake Engineering, paper 0318, New Zealand 2000.

[13] Adachi, Y., Ishizaki, H., Ikehata, S., Ikeda, S. : Verification of the Failure of Reinforced Concrete Piers under the Near-field Earthquake. Hanshin Expressway Public Corporation Publications, Japan, 2003.

[14] Bielak, J.: "Dynamic response of non-linear building-foundation systems". Earthquake Engineering and Structural Dynamics, Vol. 6, No. 1, pp 17-30, Jan.-Feb. 1978.

[15] Resendiz, D. and Roesset, J.M.: "Soil-structure interaction in Mexico City during the 1985 earthquake". The Mexico Earthquakes of 1985, ASCE Special Publication, M. A. Cassaro & E. M. Romero (eds.), pp. 193 – 203, 1987.

[16] Meymand, P.J.: "Shaking table scale model tests of nonlinear soil-pile-superstructure interaction in soft clay". Ph.D. Dissertation, University of California, Berkeley, 1998.

[17] Takewaki, I.: "Remarkable response amplification of building frames due to resonance with the surface ground". Soil Dynamics and Earthquake Engineering, Vol. 17, pp. 211-218, 1998

[18] Mylonakis, G. and Gazetas, G.: "Seismic soil-Structure Interaction: Beneficial or Detrimental ? ". Journal of Earthquake Engineering, Vol 4, No 3, pp. 277-301, 2000.

[19] Syngros, C.: "Seismic response of piles and pile-supported bridge piers evaluated through case histories". Ph.D. Dissertation , City University of New York , 2004.

[20] Gazetas, G.: Foundation vibrations. Foundation Engineering Handbook H.Y. Fang, ed., Van Nostrand Reinholds, 553-593, 1991.

[21] Mylonakis, G., Nikolaou, A., and Gazetas, G.: "Soil-pile-bridge seismic interaction: kinematic and inertial effects. Part I : Soft soil ". Earthquake Engineering & Structural Dynamics, Vol. 26, pp. 337-359, 1997.

[22] Poulos, H.G. & Davis, E.H.: Pile foundation analysis and design. Jonh Wiley & Sons, 1980.

[23] Michaelides, O. and Gazetas G.: "Non-linear analysis of piles". Research Report of Soil Mechanics Laboratory, National Technical University of Athens, 1998.

[24] Gazetas, G. and Dobry, R.: " Horizontal response of piles in layered soils" . Journal of Geotechnical Engineering, Vol .110, No. 1, pp. 20-21, 1984.

[25] Somerville P. : "Seismic Hazard Evaluation State-of-the–Art Paper". 12th World Conference on Earthquake Engineering, New Zealand, Vol. 3, pp. 325–346, 2000